Journal of Materials Chemistry B

ROYAL SOCIETY OF CHEMISTRY

COMMUNICATION

View Article Online
View Journal | View Issue

Cite this: J. Mater. Chem. B, 2023, 11, 5748

Received 24th March 2023,
Accepted 25th May 2023

DOI: 10.1039/d3tb00629h

rsc.li/materials-b

Synergistic antibacterial action of lignin-squaraine hybrid photodynamic therapy: advancing towards effective treatment of antibiotic-resistant bacteria†

Ferdinandus, ‡[a] Chaemin Joo, ‡[a] Dan Kai [bc] and Chi-Lik Ken Lee *[ac]

Antibacterial photodynamic therapy (aPDT) is emerging as an effective means of treating pathogenic bacteria, especially in light of the challenges posed by antibiotic resistance. SQR29, an organophotosensitizer, was encapsulated in a poly(lignin/PEG/PPG urethane) hydrogel to enable targeted treatment at a specific infected area. The hydrogel exhibited free radical scavenging properties which were effective in preventing oxidative stress and promoted wound healing. The hydrogel exhibited a significant aPDT effect on Gram-positive bacteria, hence showing its potential in combating antibiotic-resistant pathogenic bacteria in chronic wound infection.

The increasing global prevalence of antibiotic-resistant bacteria raises a significant public health concern, as the rate of infections caused by these bacteria continues to escalate, particularly in developing countries where antibiotics are being used excessively and inappropriately.[1] For instance, *Staphylococcus aureus* (*S. aureus*) has been reported to show resistance against methicillin which has led to almost 120 000 blood-borne infections and 20 000 related deaths in the United States in 2017.[2] Bacterial infections in wounds have been found to cause prolonged inflammatory response and significant damage to endothelial function, which plays a critical role in angiogenesis, and hence contributing to the delay of the wound healing process.[3]

Antimicrobial photodynamic therapy (aPDT) is a localized treatment to combat antibacterial resistance.[4] aPDT involves the use of visible light of a specific wavelength to excite photosensitizers (PS) to generate reactive oxygen species (ROS) that can induce oxidative stress, which is known to kill bacteria.[4] This allows aPDT to be applied exclusively to localized infections, since illumination of visible light to living tissues is a relatively localized process.

Asymmetric squaraine (SQR) dyes possess many attractive photophysical properties such as strong absorption in the visible to far-red region.[5,6] In this study, SQR29 was found to possess photodynamic properties, and was used as an organophotosensitizer (Fig. 1 and Table S1, ESI†).[7] However, SQR29 has several limitations including toxicity, solubility issues and dye aggregation that can result in fluorescence quenching.[8]

To overcome these limitations, aPDT for localized infections can be carried out by delivery of SQR29 to the infected area *via* a hydrogel. Hydrogels possess a variety of attractive properties such as high biocompatibility, biodegradability, and the ability to encapsulate drugs and proteins.[9–13] In this report, poly(lignin/PEG/PPG urethane) (Lignin-PEG-PPG) is utilized due to its ability to form micelles in aqueous solution which enables encapsulation of SQR29 (Fig. 1).[14]

Lignin-PEG-PPG was synthesized *via* polyaddition coupling with hexamethylene diisocyanate (HDMI) as the cross-linking agent. Lignin-PEG-PPG is a triblock copolymer made up of (1) hydrophilic polyethylene glycol (PEG), (2) thermosensitive polypropylene glycol (PPG) and (3) biodegradable hydrophobic lignin (Fig. 1).[15] Lignin-PEG-PPG hydrogel micellization process is known to be entropy driven.[15] An increase in temperature will lead to simultaneous formation of micelles and encapsulation of the hydrophobic SQR29 dyes in the environment (Fig. 1). The derived poly(lignin/PEG/PPG urethane) loaded with SQR29 is referred to as LSQR29.

Hydrogels have several advantages compared to traditional dressing such as cotton or bandages which has gained considerable interest in wound care as they exhibit similar physiochemical properties to natural tissue owing to their high-water content, allowing them to maintain a moist wound environment to prevent tissue dehydration, cell death and promote angiogenesis and collagen synthesis.[3,13,16] In the inflammation stage, wounds naturally produce ROS for bactericidal effects but excessive accumulation of oxygen free radicals in wounds can cause increased permeability of cell capillary walls, leading to damage in the endothelial cells which can promote cell

[a] School of Chemistry, Chemical Engineering and Biotechnology, Nanyang Technological University, 21 Nanyang Link, Singapore 637371, Singapore
[b] Institute of Materials Research and Engineering (IMRE), Agency for Science, Technology, and Research (A*STAR), 2 Fusionopolis Way, Innovis, #08-03, Singapore 138634, Singapore
[c] Institute of Sustainability for Chemicals, Energy and Environment (ISCE²), Agency for Science, Technology, and Research (A*STAR), 1 Pesek Road, Singapore 627833, Singapore. E-mail: ken_lee@isce2.a-star.edu.sg

† Electronic supplementary information (ESI) available. See DOI: https://doi.org/10.1039/d3tb00629h

‡ These authors contributed equally to this work.

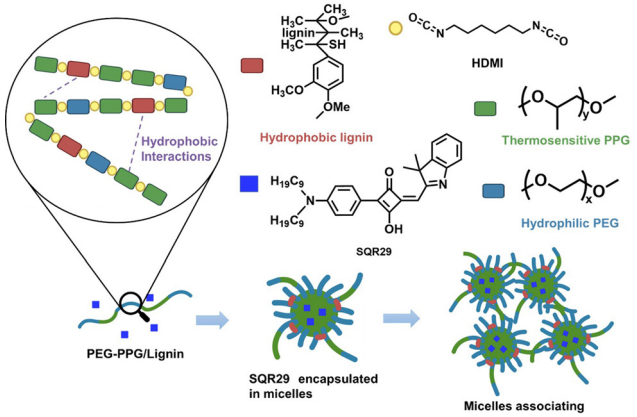

Fig. 1 Schematic representation of the micelle association model between Lignin-PEG-PPG and SQR29.

necrosis.[17,18] Lignin is known to be an oxygen free radical scavenger as it contains many aromatic moieties which makes it resistant to oxidation.[16] By incorporating lignin into the hydrogel, lignin can be applied directly onto the wound site, hence enhancing the effectiveness of lignin as an antioxidant and promoting wound healing. Upon irradiation, SQR29 encapsulated in Lignin-PEG-PPG exhibits strong efficacy in photodynamic therapy to eradicate bacterial infection. Without irradiation, the hydrogel acts as an oxygen radical scavenging agent to promote wound healing (Fig. 2).

ROS generation by LSQR29 was determined by dichlorodihydrofluorescein (DCF) assay. Presence of ROS will result in oxidation of dichlorodihydrofluorescein (H_2DCF) to produce DCF substrate which emits green fluorescence. H_2DCF substrate was directly used for the *in vitro* assay. The commercially available pluronic F127 (PF127) with a similar PEG-PPG block structure and thermogelation mechanism was implemented as the negative control in this study.[14] The fold change of fluorescence intensity of DCF by Lignin-PEG-PPG and PF127 was minimal, indicating that the production of ROS upon irradiation was very low. The highest fold change of 145 was observed in SQR29 (65 μM) followed by LSQR29 (65 μM) at 106 (Fig. 3A). The observed reduction in ROS levels in LSQR29 may be attributed to the radical scavenging activity of lignin.

S. aureus (Gram-positive) and *Escherichia coli* (*E. coli*, Gram-negative) are frequently associated with wound infection and

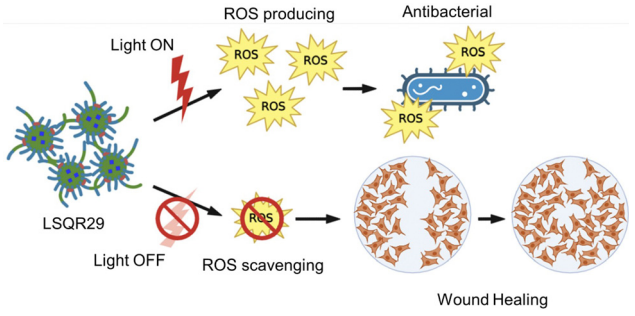

Fig. 2 Schematic illustration of LSQR29 with multifunctional properties.

can significantly impede the healing process.[3] A live/dead cell assay by propidium iodide (PI) staining of treated and untreated microbial strains were performed to investigate the antimicrobial effect of both free and encapsulated SQR29. Hoechst can easily cross the bacterial cell membrane to stain the DNA of both live and dead cells, hence it was used to label the total number of bacterial cells in the confocal laser scanning microscopy (CLSM) images.[19] PI only entered dead bacteria through their damaged cellular membrane. Intracellular PI binds to bacteria DNA and emits a red fluorescence.[16] Untreated bacteria images showed mostly unstained viable cells, indicating no observable antibacterial effect, while those treated with Lignin-PEG-PPG and PF127 displayed very minimal red fluorescence. This shows that lignin is not a contributing factor to the antibacterial effects exhibited by LSQR29. Treatment of bacteria with SQR29 (65 μM) and LSQR29 (65 μM) both exhibited significant red fluorescence which suggests remarkable cell death after the aPDT treatment. *S.aureus* demonstrated a higher antibacterial rate of 100% for SQR29 and 97.0% for LSQR29 while *E. coli* had antibacterial rate of 100% for SQR29 and 75.8% for LSQR29 (Fig. 3B–E).

Plate counting assay was conducted to further investigate the antibacterial activities of SQR29 and LSQR29. The number of bacterial colonies were much lower in the SQR29 and LSQR29 treated groups compared to the blank control, Lignin-PEG-PPG and PF127 groups. Quantitative analysis of the bacterial colony forming units (CFU) showed that LSQR29 was effective in inhibiting the growth of *S. aureus* and *E. coli*, with antibacterial rates of 83.0% and 75.9% respectively. (Fig. 3F–H).

The effect of aPDT on Gram-positive and Gram-negative bacteria can differ due to their varying levels of susceptibility.[20] *S.aureus* has a relatively porous cell wall, consisting of a thick peptidoglycan layer which promotes adhesion of the sugar contents found within lignin. This increased proximity of the encapsulated SQR29 to the bacteria enables ROS to exert its bactericidal effects more efficiently.[21] On the other hand, *E. coli* have an additional outer membrane surrounding a thin layer of peptidoglycan which can hinder the adhesion of the lignin to the bacterial cell wall, hence increasing the resistance of *E. coli* to APDT.[22]

The antioxidant activities of LSQR29 were evaluated by the 2,2-di(4-*tert*-octylphenyl)-1-picrylhydrazyl (DPPH) assay. Lignin-PEG-PPG and LSQR29 displayed good antioxidant activity of 84.0% and 95.0% after 24 h of incubation. In contrast, PF127 (control) showed a lower antioxidant activity of 63.0%, implying that the antioxidant properties of the hydrogel were attributed to the lignin within it (Fig. 4A).

A scratch assay was subsequently conducted to investigate the potential of LSQR29 in promoting *in vitro* wound healing. After 24 h and 48 h of treatment, mouse fibroblast 3T3 cells treated with Lignin-PEG-PPG and LSQR29 exhibited significantly improved cell migration and wound closure compared to the untreated control group. This indicates that the radical scavenging and wound-closing properties of the hydrogel was not hindered by the encapsulation of SQR29. It can be observed that PF127 did not demonstrate a noticeable effect on promoting cell migration compared to the control group (Fig. 4B and C).

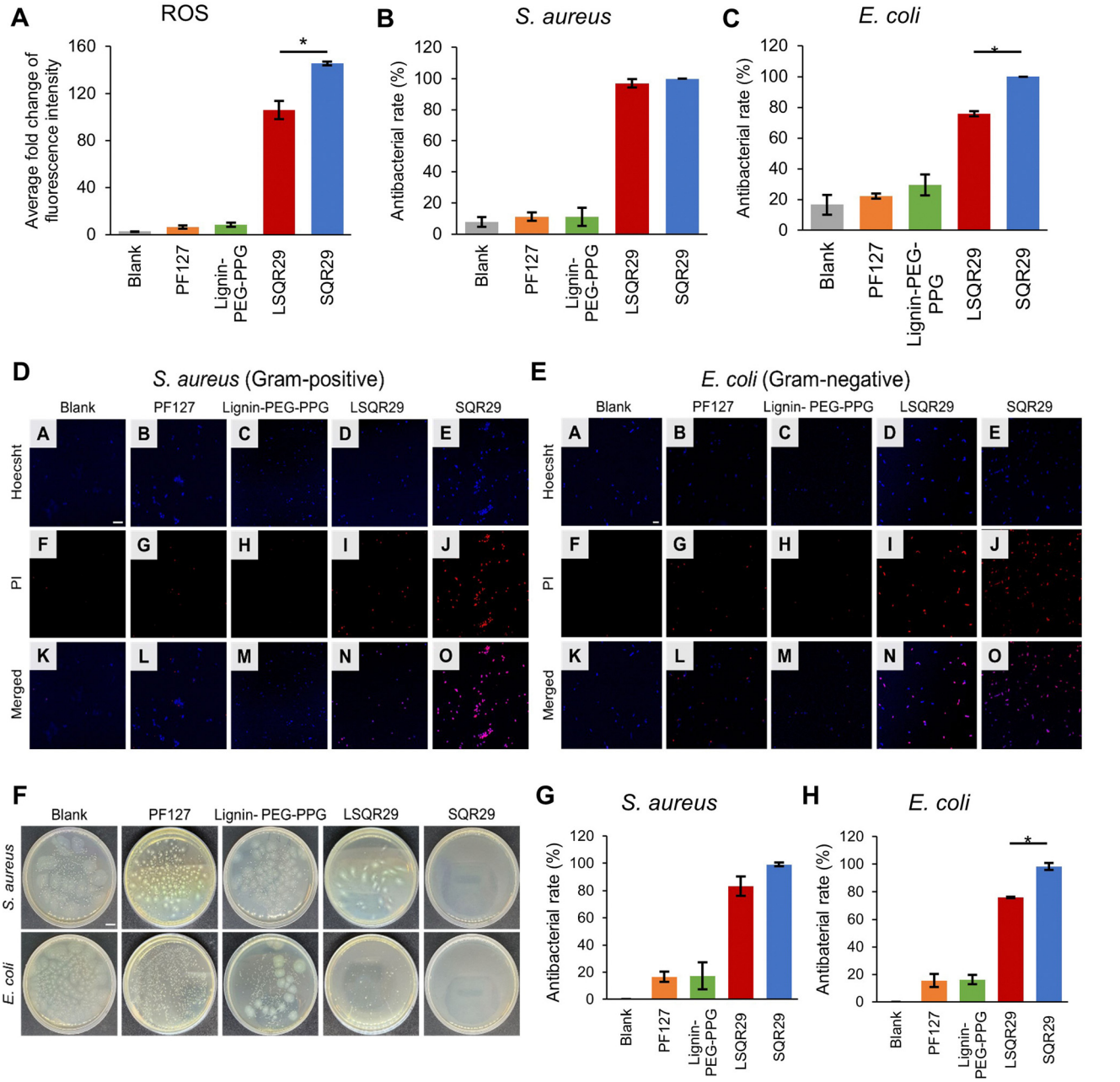

Fig. 3 (A) Fold change of fluorescence intensity before and after irradiation. (B) and (C) Antibacterial rate of treated and untreated *S. aureus* and *E. coli* obtained from CLSM images. (D) and (E) CLSM images of treated and untreated *S. aureus* and *E. coli*. Panels A–E shows bacteria stained by Hoechst, Panels F–J shows dead bacteria stained by propidium iodide (PI), Panels K–L shows the merged images of bacteria. Scale = 10 μm. (F) Representative images of CFUs of *S. aureus* and *E. coli*. Scale = 100 mm. (G) and (H) Antibacterial rates of *S. aureus* and *E. coli* from counting the colonies in (F). *$p < 0.05$ *versus* PF127 (control). All samples were measured in triplicate.

In conclusion, SQR29 was encapsulated into poly(lignin/PEG/PPG urethane) to form a hydrogel (LSQR29) which can provide excellent photodynamic properties. LSQR29 displays exceptional antibacterial properties owing to the high levels of ROS produced upon irradiation. aPDT was especially effective against Gram-positive bacteria compared to Gram-negative due to the microbial strains' differing morphology. Furthermore, LSQR29 had excellent biocompatibility and oxygen free radical abilities to promote *in vitro* wound healing. Thus, the hybrid hydrogel shows promise as an alternative therapeutic agent against antibiotic-resistant microbial pathogens and has potential for use as a wound dressing to promote wound healing in near future.

Author contributions

F.: conceptualization, formal analysis, investigation, methodology, validation, visualization, and writing – original draft. C. M. J.: conceptualization, data curation, formal analysis, investigation, methodology, validation, visualization, and writing – original

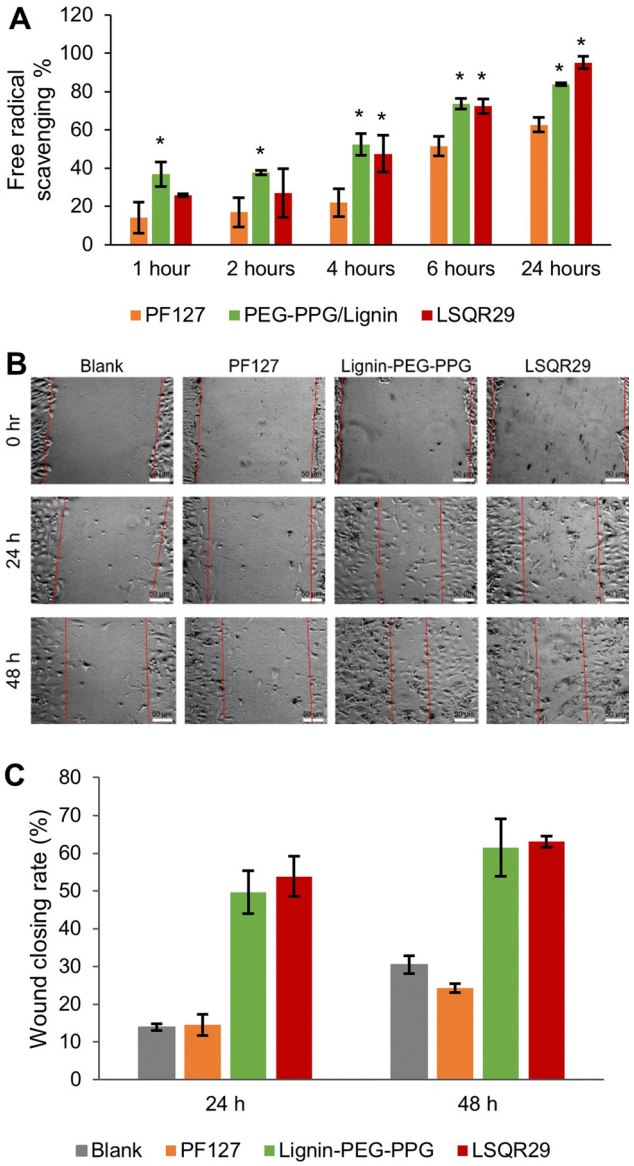

Fig. 4 (A) Free radical scavenging as a measurement of antioxidant activity, $*p < 0.05$ *versus* PF127 (control). (B) Images of wound healing in different groups of treatment and control group at 0 h, 24 h and 48 h. Scale = 50 μm. (C) Percent (%) wound closing rate of treated and untreated 3T3 cells after 24 h and 48 h. All samples were measured in triplicate.

draft. D. K.: conceptualization and resources. C. L. K. L.: conceptualization, formal analysis, funding acquisition, investigation, methodology, project administration, supervision, validation, visualization, and writing – original draft.

Conflicts of interest

There are no conflicts to declare.

Acknowledgements

The research was conducted as a part of NICES (NTU-IMRE Chemistry Lab for Eco Sustainability), a joint research initiative between Nanyang Technological University, School of Chemistry, Chemical Engineering and Biotechnology (NTU CCEB) and Institute of Materials Research and Engineering, from Agency for Science, Technology, and Research (IMRE A*STAR) under joint research grant for Sustainable Materials (No. 021614-00001).

Notes and references

1 R. Zhang, Y. Li, M. Zhou, C. Wang, P. Feng, W. Miao and H. Huang, *ACS Appl. Mater. Interfaces*, 2019, **11**(30), 26711–26721.
2 A. P. Kourtis, K. Hatfield, J. Baggs, Y. Mu, I. See, E. Epson, J. Nadle, M. A. Kainer, G. Dumyati, S. Petit, S. M. Ray, D. Ham, C. Capers, H. Ewing, N. Coffin, L. C. McDonald, J. Jernigan and D. Cardo, *MMWR Morb. Mortal. Wkly. Rep.*, 2019, **68**(9), 214–219.
3 Q. Ding, T. Sun, W. Su, X. Jing, B. Ye, Y. Su, L. Zeng, Y. Qu, X. Yang, Y. Wu, Z. Luo and X. Guo, *Adv. Healthcare Mater.*, 2022, **11**(12), 2102791.
4 N. E. Eleraky, A. Allam, S. B. Hassan and M. M. Omar, *Pharmaceutics*, 2020, **12**(2), 142.
5 Ferdinandus, J. R. Tan, J. H. Lim, S. Arai, K. Sou and C. L. K. Lee, *Analyst*, 2022, **147**(15), 3570–3577.
6 J. R. Tan, Ferdinandus, B. Xing and C. L. K. Lee, *Sens. Actuators, B*, 2022, **367**, 132123.
7 D. S. Lee, C. S. Kim, N. Iqbal, G. S. Park, K. Son and E. J. Cho, *Org. Lett.*, 2019, **21**(24), 9950–9953.
8 K. Ilina, W. M. MacCuaig, M. Laramie, J. N. Jeouty, L. R. McNally and M. Henary, *Bioconjugate Chem.*, 2019, **31**(2), 194–213.
9 Q. Lin, J. Y. Lim, K. Xue, X. Su and X. J. Loh, *Biomaterials*, 2021, **268**, 120547.
10 S. S. Liow, Q. Dou, D. Kai, A. A. Karim, K. Zhang, F. Xu and X. J. Loh, *ACS Biomater. Sci. Eng.*, 2016, **2**(3), 295–316.
11 E. Ye, P. L. Chee, A. Prasad, X. Fang, C. Owh, V. J. J. Yeo and X. J. Loh, *In Situ Gelling Polymers*, 2015, **17**(4), 107–125.
12 Q. Q. Dou, S. S. Liow, E. Ye, R. Lakshminarayanan and X. J. Loh, *Adv. Healthcare Mater.*, 2014, **3**(7), 977–988.
13 J. H. Lim, D. Kai and C. L. K. Lee, *New J. Chem.*, 2023, **47**, 550–553.
14 P. L. Chee, S. Sugiarto, Y. Yu, Y. C. Tan, E. Ye, D. Kai and X. J. Loh, *Macromol. Chem. Phys.*, 2022, **223**(2), 2100364.
15 O. Cally, D. J. Young and X. J. Loh, *Biodegradable Thermogels*, 2018, 1–22.
16 J. Xu, J. J. Xu, Q. Lin, L. Jiang, D. Zhang, Z. Li, B. Ma, C. Zhang, L. Li, D. Kai, H.-D. Yu and X. J. Loh, *ACS Applied Bio Materials*, 2020, **4**(1), 3–13.
17 C. Xian, Z. Gu, G. Liu and J. Wu, *Chin. Chem. Lett.*, 2020, **31**(6), 1612–1615.
18 O. Blokhina, E. Virolainen and V. Kurt, *Ann. Bot.*, 2003, **91**(5), 179–194.
19 C. Lema, A. Varela-Ramirez and R. J. Aguilera, *Curr. Cell. Biochem.*, 2011, **1**(1), 1–14.
20 Y. Nitzan, M. Gutterman, Z. Malik and B. Ehrenberg, *Photochem. Photobiol.*, 1992, **55**, 89–96.
21 D. M. Rocca, J. P. Vanegas, K. Fournier, M. C. Becerra, J. C. Scaiano and A. E. Lanterna, *RSC Adv.*, 2018, **8**(70), 40454–40463.
22 A. G. Morena and T. Tzanov, *Nanoscale Adv.*, 2022, **4**, 4447–4469.